JACS
JOURNAL OF THE AMERICAN CHEMICAL SOCIETY

COMMUNICATION

pubs.acs.org/JACS

From Metal–Organic Framework to Nanoporous Carbon: Toward a Very High Surface Area and Hydrogen Uptake

Hai-Long Jiang,[†] Bo Liu,[†] Ya-Qian Lan,[†] Kentaro Kuratani,[†] Tomoki Akita,[†] Hiroshi Shioyama,[†] Fengqi Zong,[‡] and Qiang Xu*[,†]

[†]National Institute of Advanced Industrial Science and Technology (AIST), Ikeda, Osaka 563-8577, Japan

[‡]Analytical and Testing Center, Changzhou University, Changzhou, Jiangsu, China

Supporting Information

ABSTRACT: In this work, with a zeolite-type metal–organic framework as both a precursor and a template and furfuryl alcohol as a second precursor, nanoporous carbon material has been prepared with an unexpectedly high surface area (3405 m^2/g, BET method) and considerable hydrogen storage capacity (2.77 wt % at 77 K and 1 atm) as well as good electrochemical properties as an electrode material for electric double layer capacitors. The pore structure and surface area of the resultant carbon materials can be tuned simply by changing the calcination temperature.

Nanostructured porous carbon materials have attracted much attention because of their extensive uses as sorbents in gaseous or liquid adsorptions, catalyst supports, and electrode materials for electric double layer capacitors (EDLCs) and fuel cells.[1−3] Highly porous carbons might be prepared via a variety of methods, including activation (physical or chemical), carbonization of polymer aerogels, template synthetic procedures, and so on.[1−4] Resorcinol–formaldehyde (RF) and melamine–formaldehyde (MF) aerogels have been synthesized as precursors to afford carbon aerogels with pore characteristics tailored by adjusting the synthetic parameters.[4] Traditional inorganic porous materials, such as mesoporous silica and zeolites, have been successfully used as excellent templates for preparing mesoporous and microporous carbons, respectively, by the nanocasting technique in recent years.[2,3] Each approach has its own advantages for the formation of carbons with controlled pore texture or/and improved surface area, which are of great importance and considered to be the key factors in optimizing the performance in most applications, especially for enhancing their hydrogen uptake capacity.[5]

On the other hand, porous metal–organic frameworks (MOFs), which are emerging as a new class of crystalline porous materials with multiple functionalities, have received great interest.[6] A great deal of research effort during the past decade has mostly been aimed at preparing new MOF structures and studying their applications in gas storage and separation and in catalysis.[6−8] Porous MOFs are usually thermally robust and have nanoporous space suitable for small molecules to access and participate in "ship-in-bottle" reactions.[7e,f] Therefore, they can reasonably be used as hard templates, similar to mesoporous silica and zeolites, to allow the reactions of small carbon precursors inside the pores, affording porous carbons. Since our first work on this subject,[9a] there have been several reports on porous carbon materials with similar or lower surface areas obtained from MOF templates, in which MOF-5 (or Bi-doped MOF-5[9b]) with an air-sensitive structure or Al-PCP[9e] with low surface area were adopted.[9] On the basis of these persistent efforts, we are aware of the crucial role of the stability and pore characteristics of a MOF template in determining the pore texture of the resultant porous carbon. Meanwhile, in view of their high carbon contents, the MOFs themselves could be excellent carbon precursors. Ma et al. have very recently demonstrated that the organic moiety in MOFs can be converted to carbon.[10] It has been suggested that incorporation of nitrogen atoms into the carbon nanostructure can enhance the mechanical and energy-storage properties, among others.[11] In this work, by elaborately choosing a chemically and thermally robust as well as highly porous zeolite-type MOF (ZIF-8) as both a precursor and a template and furfuryl alcohol (FA) (molecular dimensions of 8.43 Å × 6.44 Å × 4.28 Å)[9a] as a second precursor, we have successfully prepared porous carbons with exceptionally high surface areas and hydrogen sorption capacities (close to the highest values reported to date) as well as excellent electrochemical performance as electrode materials for EDLCs. The ZIF-8 framework [$Zn(MeIM)_2$; MeIM = 2-methylimidazole],[12] involving the N-containing methylimidazole ligand, may act as a precursor to give N-doped porous carbon. In addition, it has an intersecting three-dimensional structural feature, high thermal stability (~400 °C), large pore size (diameter of 11.6 Å), and large Brunauer–Emmett–Teller (BET) surface area (1370 m^2/g), making it suitable as a template for porous carbon synthesis.

FA was first introduced into pretreated/bare ZIF-8.[13] The mixture was stirred in an evacuated environment for several hours and allowed to stir in air for up to ~24 h. After careful filtration and washing with ethanol to remove physically adsorbed FA on the surface, the FA/ZIF-8 composite was charged into a temperature-programmed furnace under an Ar flow, heat-treated at 80 °C for 24 h and then at 150 °C for 6 h, and finally calcined at 800 or 1000 °C for 8 h to afford the carbon materials designated as C800 and C1000, respectively. The FA underwent polymerization and carbonization in turn inside the pores of ZIF-8, and ZIF-8 itself was also subjected to carbonization/decomposition during the heat-treatment process (Scheme 1).

Received: April 7, 2011
Published: July 13, 2011

Scheme 1. Schematic Illustration of the Preparation Procedure for Nanoporous Carbon (The Cavity in ZIF-8 Is Highlighted in Yellow)

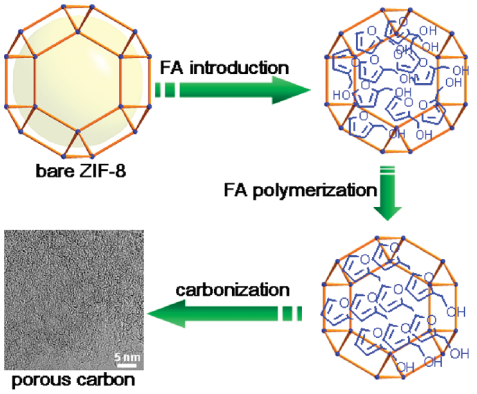

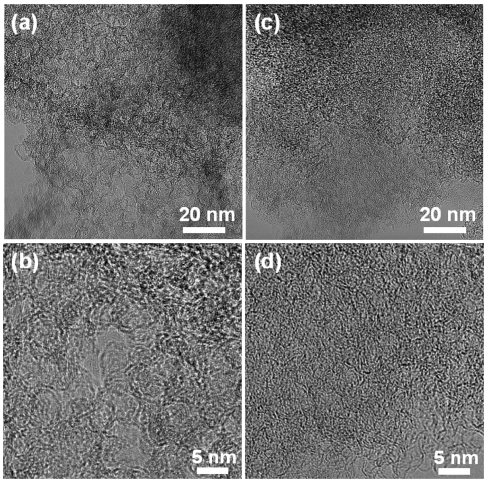

Figure 1. TEM images of samples of (a, b) C800 and (c, d) C1000 at different magnifications.

Powder X-ray diffraction (PXRD) profiles displayed only two broad peaks located at around 25 and 44° that were assigned to the carbon (002) and (101) diffractions, respectively.[13] No diffraction peaks of impurities could be observed, and the carbonization temperature was close to the boiling point of Zn metal, revealing that carbon-reduced Zn metal vaporized under the carbonization conditions. From the weak (002) peaks in the PXRD profiles, the degree of graphitization of both C800 and C1000 could be low, revealing a low concentration of parallel single layers in the obtained carbon materials.[14]

From the transmission electron microscopy (TEM) observations, apparent oriented multilayer domains and graphene sheets stacked in parallel were very few and not readily distinguishable, whereas mostly disordered graphene layer domains were observed in both samples (Figure 1), in agreement with the PXRD analysis mentioned above. Their variational textures revealed that the structures of the resultant carbon materials could be tuned by reasonably changing the calcination temperature. It is proposed that the incomplete accumulation of FA inside the MOF pores and the polymerization of FA as well as pyrolysis of polymerized FA (PFA) first produce small pores. Subsequently,

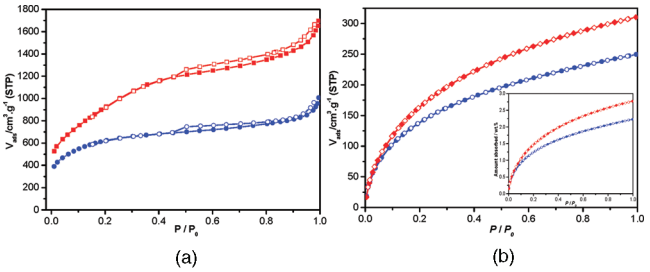

Figure 2. (a) Nitrogen and (b) volumetric hydrogen adsorption−desorption isotherms for C800 (blue) and C1000 (red) samples from 0 to 1 atm at 77 K. The inset of (b) shows gravimetric hydrogen adsorption−desorption isotherms for C800 (blue) and C1000 (red). Adsorption, solid symbols; desorption, open symbols.

the ZIF-8 framework decomposes, behaving as both a carbon precursor and a template, which further affords the pore space of the resultant carbon materials during the high-temperature carbonization process.

Nitrogen sorption experiments were performed to examine the surface areas of the C800 and C1000 materials (Figure 2a). The curves for both samples are a bit similar to the I-type isotherm, and they steeply increases at low relative pressure, suggesting the dominating micropore characteristic. Meanwhile, the slight hysteresis of the desorption curves and the durative increase of the adsorption capacity before P/P_0 = 0.4 for the C1000 sample reveal the presence of a portion containing meso/macropores. Both of these observations are supported by the pore volume analyses.[13] The BET surface area and total pore volume were found to be 2169 m^2/g and 1.50 cm^3/g, respectively, for C800.[15] Unexpectedly, a much higher BET surface area of 3405 m^2/g and corresponding pore volume of 2.58 cm^3/g were observed for C1000,[15] revealing that the carbonization temperature is critical for the structural evolution of the resultant carbon. The above BET surface areas are comparable to those based on the consistency criteria (2181 and 3453 m^2/g for C800 and C1000, respectively).[13,16] To our knowledge, the BET surface area of C1000 is close to the highest value reported to date for templated carbon materials [e.g., KUA6, ZTC, P7(2)-H, etc.],[3b−g] and much higher than those for all reported porous carbons derived from MOF templates (Table 1).[9] Control experiments showed that ZIF-8 as the only precursor can yield porous carbon with a surface area of up to 3148 m^2/g,[13] which is the first report to date of carbon materials with such high surface area derived from a MOF precursor.[10] Upon introduction and polymerization of FA in ZIF-8, the PFA/ZIF-8 composite affords a higher surface area of the carbon product. The results indicate that ZIF-8 makes the main contribution while the addition of the FA precursor can reasonably improve the pore texture of the resultant carbon.

Encouraged by the high surface area, we also conducted hydrogen uptake measurements at 77 K. As shown in Figure 2b, the hydrogen storage capacities of C800 and C1000 at 1 atm reached 2.23 and 2.77 wt %, respectively. The hydrogen uptake capacity of C1000 is much higher than that of ZIF-8 (~140 cm^3/g STP at 1 bar)[12a] and also among the highest values ever reported for activated carbon materials as far as we know.[1f,3c,3d] The isotherms do not exhibit any hysteresis, confirming that the uptake of hydrogen by the porous carbon materials is reversible. As indicated by pore size distribution analysis, the dominating micropore distribution can also be considered to benefit the high hydrogen uptake.[3h,4] Both the surface area and H_2 uptake of the

dx.doi.org/10.1021/ja203184k |J. Am. Chem. Soc. 2011, 133, 11854–11857

Table 1. Texture Parameters of Porous Carbon Materials Prepared Using MOFs as Templates/Precursors

sample	S_{BET} (m^2/g)[a]	pore volume (cm^3/g)	temp. (°C)	H_2 uptake (wt %)[b]	ref
NPC	2872	2.06	1000	2.6	9a
WMC	2587	3.14	1000	n.d.	9b
NPC_{530}	3040	2.79	530		
NPC_{650}	1521	1.48	650		
NPC_{800}	1141	0.84	800	n.d.	9c
NPC_{900}	1647	1.57	900		
NPC_{1000}	2524	2.44	1000		
MC	1812	2.87			
MPC	1543	2.49			
MAC	384	0.13	900	n.d.	9d
MC-A	1673	1.33			
MPC-A	1271	1.92			
MAC-A	2222	1.14			
Al-PCP-FA1	263	0.439	1000	n.d.	9e
Al-PCP-FA2	513	0.844			
C800	2169	1.50	800	2.23	this work
C1000	3405	2.58	1000	2.77	

[a] The specific surface area was calculated using the BET method. [b] Conditions: 77 K and 1 atm. n.d.: no data.

C1000 sample are much higher than those reported for carbon materials templated with MOF-5 or Al-PCP.[9] It is assumed that the particular air sensitivity of MOF-5[17] and low surface area of Al-PCP[18] are disadvantageous. Moreover, ZIF-8, which contains N-based ligands, is regarded to benefit the carbon formation relative to carboxylic acid-based MOFs because the latter itself should give lower carbon yields as a result of the escape of CO, CO_2, etc., during the carbonization process under an inert gas flow. The highly porous character and robust and oxygen-free framework of ZIF-8 make it suitable as both a precursor and a template for porous carbon synthesis, which could be responsible for its superior performance.

Electrochemical measurements were carried out for both carbon materials using two electrode cells without a reference electrode (electrolyte: 1 M H_2SO_4). Cyclic voltammetry is a suitable tool for estimating the difference between the non-Faradaic and Faradaic reactions and can also be used for preliminary determination of the power density and energy density of supercapacitors.[19] Figure 3a,b presents steady-state cyclic voltammograms (CVs) of C800 and C1000 supercapacitors obtained by applying a potential varying from −0.5 to 0.5 V at different sweep rates (1−500 mV/s). The regular rectangular shapes without any redox peaks reveal their excellent capacitive behavior. The current responses of both supercapacitors show a slight sweep-rate dependence. As only the accessible surface area contributes to the capacitance, it is reasonable to consider that the specific capacitance is contributed by meso/macropores of the active carbon materials at high sweep rates and by micropores at lower sweep rates. The specific capacitance decayed by ∼15%

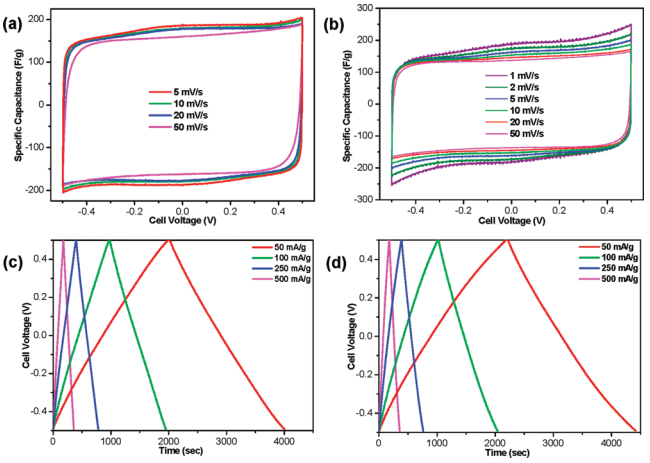

Figure 3. (a, b) CVs at different scan rates and (c, d) galvanostatic charge−discharge profiles at different current densities for (a, c) C800 and (b, d) C1000 samples.

(from 188 to 160 F/g for C800 and 161 to 137 F/g for C1000) as the sweep rate increased from 5 to 50 mV/s, indicating their excellent mesoporosity characteristics, in agreement with the pore size distribution analysis.[13] The results are higher than those for the reported carbon materials templated from classical mesporous silica, such as SBA-15[20a] and SBA-16,[20b] and comparable to those for reported MOF-templated carbons.[9] The observed slight increase in specific capacitance from 173 F/g (2 mV/s) to 188 F/g (1 mV/s) is possibly due to the diffusion limitation within the micropores in the carbon material of C1000. The applicability of supercapacitors can be directly evaluated by means of the galvanostatic charge−discharge method. Plots of voltage versus time for the C800 and C1000 supercapacitors at different current densities of 50−500 mA/g are displayed in Figure 3c,d. As expected, the discharge curves of both carbon capacitors are symmetric with the corresponding charge curves. The typical triangular profiles confirm good electrochemical capacitive properties of both carbon materials. The specific capacitances are ∼200 F/g for both supercapacitors at a current density of 250 mA/g.

In conclusion, we have successfully prepared porous carbon materials with very high surface areas and hydrogen uptake capacities as well as good electrochemical properties as electrode materials by employing a robust N-containing MOF (ZIF-8) as both a precursor and a template and FA as the other precursor via an easily handled method. Only a limited amount of the FA precursor could be effectively loaded because of the small pores in ZIF-8, but nevertheless, this work unambiguously shows the great potential of carbon materials derived from porous MOFs in energy-storage applications, which opens up an avenue to enrich the functional applications of porous MOFs as one of the fastest growing fields. With the great number of available MOF structures, MOF-based porous carbon materials with tailorable pore textures and improvable performances could be highly promising. In-depth studies of MOF-derived carbon materials are in progress in our group.

■ ASSOCIATED CONTENT

Supporting Information. Full sample preparation details, characterization data, and discussions. This material is available free of charge via the Internet at http://pubs.acs.org.

AUTHOR INFORMATION

Corresponding Author
q.xu@aist.go.jp

ACKNOWLEDGMENT

The authors thank Prof. Joseph T. Hupp and the reviewers for their constructive suggestions, Prof. Randall Q. Snurr and Dr. Youn-Sang Bae for fruitful discussions on consistency criteria for calculating BET surface area, AIST and JSPS for financial support, and Mr. K. Washio at Shimadzu Corporation (Japan) for kind help with the pore volume analysis. H.-L.J. thanks JSPS for a postdoctoral fellowship.

REFERENCES

(1) (a) Flandrois, S.; Simon, B. *Carbon* **1999**, *37*, 165. (b) Kyotani, T. *Carbon* **2000**, *38*, 269. (c) Hu, Z.; Srinivasan, M. P.; Ni, Y. *Adv. Mater.* **2000**, *12*, 62. (d) Ryoo, R.; Joo, S. H.; Kruk, M.; Jaroniec, M. *Adv. Mater.* **2001**, *13*, 677. (e) Lee, J.; Kim, J.; Hyeon, T. *Adv. Mater.* **2006**, *18*, 2073. (f) Thomas, K. M. *Catal. Today* **2007**, *120*, 389. (g) Yang, R. T.; Wang, Y. *J. Am. Chem. Soc.* **2009**, *131*, 4224. (h) Hu, B.; Wang, K.; Wu, L.; Yu, S.-H.; Antonietti, M.; Titirici, M.-M. *Adv. Mater.* **2010**, *22*, 813.

(2) (a) Wu, C. G.; Bein, T. *Science* **1994**, *266*, 1013. (b) Joo, S. H.; Choi, S. J.; Oh, I.; Kwak, J.; Liu, Z.; Terasaki, O.; Ryoo, R. *Nature* **2001**, *412*, 169. (c) Lu, A.; Kiefer, A.; Schmidt, W.; Schüth, F. *Chem. Mater.* **2004**, *16*, 100. (d) Tanaka, S.; Nishiyama, N.; Egashira, Y.; Ueyama, K. *Chem. Commun.* **2005**, 2125. (e) Liang, C.; Li, Z.; Dai, S. *Angew. Chem., Int. Ed.* **2008**, *47*, 3696.

(3) (a) Johnson, S. A.; Brigham, E. S.; Ollivier, P. J.; Mallouk, T. E. *Chem. Mater.* **1997**, *9*, 2448. (b) Ma, Z.; Kyotani, T.; Liu, Z.; Terasaki, O.; Tomita, A. *Chem. Mater.* **2001**, *13*, 4413. (c) Matsuoka, K.; Yamagishi, Y.; Yamazaki, T.; Setoyama, N.; Tomita, A.; Kyotani, T. *Carbon* **2005**, *43*, 855. (d) Jordá-Beneyto, M.; Suárez-García, F.; Lozano-Castelló, D.; Cazorla-Amorós, D.; Linares-Solano, A. *Carbon* **2007**, *45*, 293. (e) Nishihara, H.; Hou, P.-X.; Li, L.-X.; Ito, M.; Uchiyama, M.; Kaburagi, T.; Ikura, A.; Katamura, J.; Kawarada, T.; Mizuuchi, K.; Kyotani, T. *J. Phys. Chem. C* **2009**, *113*, 3189. (f) Hou, P.-X.; Yamazakia, T.; Orikasa, H.; Kyotani, T. *Carbon* **2005**, *43*, 2624. (g) Yang, Z.; Xia, Y.; Mokaya, R. *J. Am. Chem. Soc.* **2007**, *129*, 1673. (h) Xia, Y.; Walker, G. S.; Grant, D. M.; Mokaya, R. *J. Am. Chem. Soc.* **2009**, *131*, 16493. (i) Itoi, H.; Nishihara, H.; Kogure, T.; Kyotani, T. *J. Am. Chem. Soc.* **2011**, *133*, 1165. (j) Xia, Y.; Yang, Z.; Mokaya, R. *Nanoscale* **2010**, *2*, 639.

(4) (a) Horikawa, T.; Hayashi, J.; Muroyama, K. *Carbon* **2004**, *42*, 1625. (b) Matsuoka, T.; Hatori, H.; Kodama, M.; Yamashita, J.; Miyajima, N. *Carbon* **2004**, *42*, 2329.

(5) (a) Texier-Mandoki, N.; Dentzer, J.; Piquero, T.; Saadallah, S.; David, P.; Vix-Guterl, C. *Carbon* **2004**, *42*, 2744. (b) Gogotsi, Y.; Dash, R. K.; Yushin, G.; Yildirim, T.; Laudisio, G.; Fischer, J. E. *J. Am. Chem. Soc.* **2005**, *127*, 16006. (c) Yushin, G.; Dash, R.; Jagiello, J.; Fischer, J. E.; Gogotsi, Y. *Adv. Funct. Mater.* **2006**, *16*, 2288.

(6) (a) Long, J. R.; Yaghi, O. M. *Chem. Soc. Rev.* **2009**, *38*, 1213. (b) Jiang, H.-L.; Xu, Q. *Chem. Commun.* **2011**, *47*, 3351. (c) Chen, B.; Xiang, S.; Qian, G. *Acc. Chem. Res.* **2010**, *43*, 1115. (d) Farha, O. K.; Hupp, J. T. *Acc. Chem. Res.* **2010**, *43*, 1166.

(7) (a) Seo, J. S.; Whang, D.; Lee, H.; Jun, S. I.; Oh, J.; Jeon, Y. J.; Kim, K. *Nature* **2000**, *404*, 982. (b) Furukawa, H.; Ko, N.; Go, Y. B.; Aratani, N.; Choi, S. B.; Choi, E.; Yazaydin, A. Ö.; Snurr, R. Q.; O'Keeffe, M.; Kim, J.; Yaghi, O. M. *Science* **2010**, *329*, 424. (c) Kitagawa, S.; Kitaura, R.; Noro, S. *Angew. Chem., Int. Ed.* **2004**, *43*, 2334. (d) Férey, G.; Mellot-Draznieks, C.; Serre, C.; Millange, F.; Dutour, J.; Surblé, S.; Margiolaki, I. *Science* **2005**, *309*, 2040. (e) Pan, L.; Liu, H.; Lei, X.; Huang, X.; Olson, D. H.; Turro, N. J.; Li, J. *Angew. Chem., Int. Ed.* **2003**, *42*, 542. (f) Uemura, T.; Yanai, N.; Kitagawa, S. *Chem. Soc. Rev.* **2009**, *38*, 1228.

(8) (a) Pan, L.; Parker, B.; Huang, X. Y.; Olson, D. H.; Lee, J.; Li, J. *J. Am. Chem. Soc.* **2006**, *128*, 4180. (b) Mulfort, K. L.; Hupp, J. T. *J. Am. Chem. Soc.* **2007**, *129*, 9604. (c) Yang, S. J.; Choi, J. Y.; Chae, H. K.; Cho, J. H.; Nahm, K. S.; Park, C. R. *Chem. Mater.* **2009**, *21*, 1893. (d) Jiang, H.-L.; Tastu, Y.; Lu, Z.-H.; Xu, Q. *J. Am. Chem. Soc.* **2010**, *132*, 5586. (e) Ma, S. Q.; Zhou, H. C. *Chem. Commun.* **2010**, *46*, 44. (f) Xiang, S. C.; Zhou, W.; Gallegos, J. M.; Liu, Y.; Chen, B. *J. Am. Chem. Soc.* **2009**, *131*, 12415.

(9) (a) Liu, B.; Shioyama, H.; Akita, T.; Xu, Q. *J. Am. Chem. Soc.* **2008**, *130*, 5390. (b) Yuan, D.; Chen, J.; Tan, S.; Xia, N.; Liu, Y. *Electrochem. Commun.* **2009**, *11*, 1191. (c) Liu, B.; Shioyama, H.; Jiang, H.-L.; Zhang, X.-B.; Xu, Q. *Carbon* **2010**, *48*, 456. (d) Hu, J.; Wang, H.; Gao, Q.; Guo, H. *Carbon* **2010**, *48*, 3599. (e) Radhakrishnan, L.; Reboul, J.; Furukawa, S.; Srinivasu, P.; Kitagawa, S.; Yamauchi, Y. *Chem. Mater.* **2011**, *23*, 1225.

(10) Ma, S.; Goenaga, G. A.; Call, A. V.; Liu, D.-J. *Chem.—Eur. J.* **2011**, *17*, 2063.

(11) Jin, X.; Balasubramanian, V. V.; Selvan, S. T.; Sawant, D. P.; Chari, M. A.; Lu, G. Q.; Vinu, A. *Angew. Chem., Int. Ed.* **2009**, *48*, 7884.

(12) (a) Park, K. S.; Ni, Z.; Côté, A. P.; Choi, J. Y.; Huang, R.; Uribe-Romo, F. J.; Chae, H. K.; O'Keeffe, M.; Yaghi, O. M. *Proc. Natl. Acad. Sci. U.S.A.* **2006**, *103*, 10186. (b) Huang, X. C.; Lin, Y. Y.; Zhang, J. P.; Chen, X. M. *Angew. Chem., Int. Ed.* **2006**, *45*, 1557.

(13) See the Supporting Information.

(14) (a) Liu, Y.; Xue, J. X.; Zheng, T.; Dahn, J. R. *Carbon* **1996**, *34*, 193. (b) Wang, H.; Gao, Q.; Hu, J. *J. Am. Chem. Soc.* **2009**, *131*, 7016.

(15) The BET surface area and pore volume data were obtained with ASAP2010 adsorption equipment using the data in the relative pressure range 0.05−0.20.

(16) (a) Bae, Y.-S.; Yazaydın, A. Ö.; Snurr, R. Q. *Langmuir* **2010**, *26*, 5475. (b) Rouquerol, J.; Llewellyn, P.; Rouquerol, F. *Stud. Surf. Sci. Catal.* **2007**, *160*, 49.

(17) Kaye, S. S.; Dailly, A.; Yaghi, O. M.; Long, J. R. *J. Am. Chem. Soc.* **2007**, *129*, 14176.

(18) Comotti, A.; Bracco, S.; Sozzani, P.; Horike, S.; Matsuda, R.; Chen, J.; Takata, M.; Kubota, Y.; Kitagawa, S. *J. Am. Chem. Soc.* **2008**, *130*, 13664.

(19) Xing, W.; Qiao, S. Z.; Ding, R. G.; Li, F.; Lu, G. Q.; Yan, Z. F.; Cheng, H. M. *Carbon* **2006**, *44*, 216.

(20) (a) Wang, D.-W.; Li, F.; Liu, M.; Cheng, H.-M. *New Carbon Mater.* **2007**, *22*, 307. (b) Fuertes, A. B.; Lota, G.; Centeno, T. A.; Frackowiak, E. *Electrochim. Acta* **2005**, *50*, 2799.